

---

---

## Orientin attenuates pulmonary fibrosis via TGF- $\beta$ 1/suppressor of mother against decapentaplegic 3 (Smad3) pathway.

Yijin Liu<sup>1</sup> and Yao Lu<sup>2</sup>

<sup>1</sup>Department of Pharmacy, Liaoning University of Traditional Chinese Medicine Xinglin College, Shenyang, Liaoning Province, China.

<sup>2</sup>Department of Thoracic Surgery, The Fourth Affiliated Hospital of China Medical University, Shenyang City, Liaoning Province, China.

**Keywords:** Orientin; Pulmonary fibrosis; Fibroblasts; TGF- $\beta$ 1/Smad3 pathway.

**Abstract.** Orientin, a natural flavonoid found in many medicinal plants, can improve lung injury through anti-inflammatory and antioxidant effects, but its role in pulmonary fibrosis (PF) remains unstudied. Human Fetal Lung 1 (HFL1) cells were stimulated with transforming growth factor- $\beta$ 1 (TGF- $\beta$ 1), and a single intratracheal bleomycin instillation in mice was used to establish a PF mouse model. Orientin, the TGF- $\beta$ 1/suppressor of mother against decapentaplegic 3 (Smad3) pathway agonist SRI-011381, and the inhibitor SB431542 were used for intervention. The proliferation and migration were evaluated using the Cell Counting Kit-8 (CCK-8), Edu staining (evaluated proliferative activity) and a scratch-healing assay. Fibers in HFL1 cells were detected by Sirius red staining. Inflammation and fibrosis in lung tissue were assessed by pathological staining and enzyme-linked immunosorbent assay (ELISA). PF and TGF- $\beta$ 1/Smad3 pathway protein expressions were evaluated by Western blot. Orientin significantly reduced TGF- $\beta$ 1, p-Smad3, alpha-smooth muscle actin ( $\alpha$ -SMA), Collagen I, and matrix metalloproteinase (MMP)-2 levels. After Orientin treatment, the Edu positive cells, cell proliferation and migration were significantly reduced, and the number of red-stained collagen fibers was significantly reduced. After Orientin treatment, alveolar cavity collapse, inflammatory cell infiltration, and collagen fiber hyperplasia of mice were alleviated, and the contents of Hydroxyproline (HYP) and inflammatory factors in the alveolar lavage fluid were significantly reduced. SRI-011381 attenuated the effect of Orientin on the intervention, and inflammation and fibrosis levels were markedly increased. SB431542 enhanced the intervention effect of Orientin. Orientin inhibited TGF- $\beta$ 1/Smad3 signaling, inhibited fibroblast-to-myofibroblast transition (FMT) and extracellular matrix (ECM) production, and alleviated inflammatory and fibrotic damage.

## La orientina reduce la fibrosis pulmonar mediante la vía de señalización TGF- $\beta$ 1/Smad3.

*Invest Clin* 2026; 67 (2): 241 – 259

**Palabras clave:** Orientin; Fibrosis pulmonar; Fibroblastos; Vía de TGF- $\beta$ 1/Smad3.

**Resumen.** La orientina, un flavonoide natural presente en una variedad de plantas medicinales, reduce el daño pulmonar gracias a sus efectos antiinflamatorios y antioxidantes. Sin embargo, no se han reportado estudios sobre su efecto en la fibrosis pulmonar (PF). Las células Human Fetal Lung 1 (HFL1) se estimularon con el factor de crecimiento transformante  $\beta$ 1 (TGF- $\beta$ 1) y se administró una dosis única de bleomicina por vía intratraqueal para establecer un modelo de PF en ratones. La intervención se realizó con orientina, el agonista SRI-011381 de la vía supresora de madre contra el decapentapléjico 3, y el inhibidor SB431542. La proliferación y migración de células HFL1 se evaluaron mediante el Kit-8 (CCK-8) para el conteo de células, la tinción de Edu (para evaluar la actividad proliferativa) y mediante el ensayo de cicatrización de heridas. Las fibras en las células HFL1 se detectaron mediante tinción con Sirius Red. La inflamación y la fibrosis del tejido pulmonar se evaluaron mediante tinción patológica y ensayo inmunoenzimático ligado a anticuerpos (ELISA). Los niveles de expresión proteica de PF y de la vía TGF- $\beta$ 1/Smad3 se analizaron mediante Western blot. La orientina reduce significativamente los niveles de las proteínas TGF- $\beta$ 1, p-Smad3, actina alfa del músculo liso ( $\alpha$ -SMA), colágeno I y metaloproteidasa de la matriz (MMP)-2. Además, el tratamiento con orientina disminuyó significativamente las células Edu positivas, la proliferación y la migración de las células HFL1, así como la formación de fibras de colágeno teñidas de rojo. El tratamiento con orientina redujo el deterioro de la cavidad alveolar, el infiltrado de células inflamatorias y la hiperplasia de fibras colágenas en el tejido pulmonar de los ratones, y disminuyó significativamente el contenido de Hydroxyproline (HYP) y de los factores inflamatorios (TNF- $\alpha$  e IL-6) en el lavado alveolar. Sin embargo, SRI-011381 atenuó el efecto de la intervención con orientina, con un aumento significativo de los niveles de inflamación y fibrosis; el SB431542 lo acentuó. La orientina inhibe la vía de señalización TGF- $\beta$ 1/Smad3, la transición de fibroblastos a miofibroblastos (FMT) y la producción de matriz extracelular (ECM), y alivia el daño inflamatorio y fibroso.

*Received:* 05-11-2025      *Accepted:* 21-12-2025

### INTRODUCTION

The main pathological features of idiopathic pulmonary fibrosis (IPF) are destruction of the lung parenchyma and accumulation of extracellular matrix (ECM) in the pulmonary interstitial and alveolar spaces, which eventually leads to destruction of al-

veolar structure and severe impairment of lung function, ultimately resulting in death<sup>1</sup>. The median survival time of IPF patients after diagnosis is short, and the prognosis is very poor<sup>2,3</sup>. At present, anti-pulmonary fibrosis (PF) drugs and lung transplantation are the main treatment options for PF. Lung-derived problems limit lung transplantation.

pirfenidone and nintedanib are the main anti-fibrosis drugs. Studies have shown that pirfenidone and nintedanib slow the decline in lung function in IPF, but overall efficacy is limited, with issues such as significant side effects, high costs, and no improvement in survival rate<sup>3</sup>. Thus, it is vital to find safe and effective new drugs for IPF therapy.

The pathogenesis of IPF is highly complex and involves multiple mechanisms, including the inflammatory response, oxidative stress, epithelial-mesenchymal transition (EMT), and inhibition of autophagy. These mechanisms are intertwined and interact to drive IPF progression. Among them, the transforming growth factor- $\beta$ 1 (TGF- $\beta$ 1)/suppressor of mother against decapentaplegic 3 (Smad3) signaling pathway is important in regulating the PF process<sup>4,7</sup>. TGF- $\beta$ 1 is a core regulator of IPF and can promote fibrosis<sup>8</sup>. When TGF- $\beta$ 1 binds to its receptor, it can phosphorylate Smad2/3 in the cytoplasm, which in turn binds Smad2/3 to Smad4 to form a trimer, enters the nucleus, and binds to specific DNA sites, thereby regulating the expression of a series of downstream fibrosis-related genes, up-regulating alpha-smooth muscle actin ( $\alpha$ -SMA) level, promoting the abnormal deposition of fibrosis-related proteins, and increasing and promoting fibroblast proliferation. It drives the fibroblast-to-myofibroblast transition (FMT), a classical pathway of TGF- $\beta$ 1-mediated fibrosis<sup>9</sup>. Therefore, TGF- $\beta$ 1/Smad signaling can regulate the transcription and protein expressions of target genes, induce PF<sup>10</sup>. Inhibition of the TGF- $\beta$ 1/Smad3 pathway reduces PF. Sinomenine alleviates inflammatory response and reverses EMT through suppressing the TGF- $\beta$ 1/Smad3 pathway, thereby reducing PF<sup>5</sup>; inhibition of AHNK2 via suppressing the TGF- $\beta$ 1/Smad3 pathway regulates EMT and alleviates PF<sup>11</sup>; PM2.5 enhances endoplasmic reticulum stress-induced autophagy, thereby activating the TGF- $\beta$ 1/Smad3 pathway, promoting ECM overproduction, ultimately aggravating PF<sup>12</sup>. In summary, the TGF- $\beta$ 1/Smad3 is a

classic pathway that mediates organ fibrosis and dominates the progression of fibrotic diseases<sup>13</sup>.

As research into treating PF with herbal medicine deepens, monomers of herbal medicine have attracted considerable attention for their single-component nature, stable structures, and notable effects. Orientin is a natural flavonoid widely found in many medicinal plants, such as *Trollius chinensis* Bunge, *Odontosoria chinensis* J. Sm., and bamboo leaves. Modern pharmacological studies have shown that orientin has many biological properties, including anti-inflammatory, antioxidant, anti-aging, antibacterial, hepatoprotective, neuroprotective, and cardioprotective effects<sup>14, 15</sup>. Studies have shown that Orientin is a possible anti-inflammatory drug. Orientin can improve mitochondrial homeostasis, inhibit chondrocyte senescence and inflammation, and reduce osteoarthritis<sup>16</sup>. The lung is the primary tissue for orientin distribution, and orientin has been shown to alleviate acute lung injury in mice by exerting anti-inflammatory and antioxidant effects<sup>17</sup>. Therefore, we believe that orientin may be an ideal anti-PF candidate drug. However, the therapeutic effect of orientin on PF and its molecular mechanism have not been systematically elucidated.

To evaluate the therapeutic potential of orientin in PF, the effects of orientin on FMT, fibrosis, inflammatory response, and the TGF- $\beta$ 1/Smad3 signaling pathway were assessed, with pirfenidone as a positive control. This study aims to demonstrate that orientin can reduce PF through the TGF- $\beta$ 1/Smad3 signaling pathway, thereby providing an important experimental and theoretical basis for the development of safe, effective, and economical anti-PF natural drugs.

## METHODS

### Cell culture and modeling

Human embryonic lung fibroblasts HFL1 were purchased from Procell Life Technology Co., Ltd. (CL-0106, Wuhan, China).

HFL1 cells were cultured with HFL1 cell-specific culture medium (CM-0106, Procell, Ham's F-12K medium containing 1% penicillin-streptomycin and 10% fetal bovine serum) in a cell culture box (MCO-18 AIGUUV, PHCbi, Japan) at 37°C and 5% CO<sub>2</sub>. The sub-culture medium was changed every 3 days.

HFL1 cells (1×10<sup>5</sup> cells/well) in the logarithmic growth phase and in good condition were inoculated into 6-well plates and routinely cultured. The next day, after adherence, orientin (S9009, Selleck, Shanghai, China) at 0, 10, 20, 40, 80, and 160 μM was added, and cells were incubated for 24 h. Then, 10 μL of Cell Counting Kit-8 (CCK-8) solution (C0037, Beyotime, Shanghai, China) was added, and cells were incubated for 2 h. The optical density (OD) at 450 nm was measured using a microplate reader (MULTISKAN, Perkin Elmer, United States), and the cell survival rate was calculated to determine the safe concentration of orientin.

HFL1 cells were divided into the control group, the model (TGF-β1) group, the positive control (TGF-β1+pirfenidone) group, the orientin low, medium, and high concentration (TGF-β1+orientin-L, TGF-β1+orientin-M, TGF-β1+orientin-H) group, the TGF-β1/Smad3 pathway agonist (TGF-β1+orientin+SRI-011381) group, and the inhibitor (TGF-β1+orientin+SB431542) group. In the TGF-β1 group, 10 ng/mL TGF-β1 (100-21, PeproTech, USA) was added to stimulate HFL1 cells for 24 h<sup>4,5</sup>. After that, 10 μM pirfenidone (Y159865, Beyotime) was added to the TGF-β1+pirfenidone group to culture HFL1 cells for 24 h; HFL1 cells were cultured with 10, 20, and 40 μM orientin for 24 h in orientin low, medium, and high concentration groups, respectively. TGF-β1+orientin+SRI-011381 and TGF-β1+orientin+SB431542 groups were added with 10 μM SRI-011381 (Y112753, Beyotime) and SB431542 (SF7890, Beyotime) at the same time as orientin. Then CCK-8 was used to measure the OD at 450 nm and calculate cell viability.

### Edu staining

After intervention, HFL1 cells were incubated with an equal volume of 20 μM Edu working solution (C0071S, Beyotime) for 3 h. The cells were fixed with paraformaldehyde, permeabilized with 1 mL of permeabilization solution (P0097, Beyotime) for 10 min, and incubated with 0.5 mL of Click reaction solution in the dark for 30 min. The cells were stained with DAPI reagent and mounted with anti-fluorescence quenching mounting agent (0100-01, South biotech, USA). Three fields of view were selected for each well under the fluorescence microscope (ECLIPSE TI2-A, Nikon, Japan), and Edu-positive cells were counted using Image J software.

### Scratch healing experiment

HFL1 cells were inoculated into 6-well plates and cultured overnight in serum-free medium after reaching confluence. A 200 μL pipette tip was used to create vertical scratches in each well, and the culture medium was replaced. The cells were then subjected to the experimental interventions and cultured for 24 h. Images were taken under a microscope (NIKON ECLIPSE E100, Nikon) at the beginning and end of the culture, and the distance between scratches was measured using ImageJ software to calculate the scratch-healing rate.

### Sirius red staining

After the HFL1 cells were cultured, 100 μL of ice-cold methanol was added to fix the cells for 5 h, and then the ice-cold methanol in the well was discarded. Hematoxylin was added to each well for staining for 20 min, and then 200 μL of Sirius red staining solution (GC307014, Servicebio, Wuhan, China) was added. The cells were incubated in the dark for 4 h. Images were observed and collected under a microscope. The collagen fibers appeared red, and the muscle fibers appeared yellow. The area of collagen fibers was analyzed using Image J software.

### Immunofluorescence

HFL1 cells were fixed with 4% paraformaldehyde for 15 min, incubated with 100  $\mu$ L of membrane-breaking working solution for 10 min, blocked with 3% BSA (bovine serum albumin) for 30 min, and incubated with the  $\alpha$ -SMA antibody (67735-1-Ig, Proteintech, Wuhan, China) overnight at 4°C. Alexa 488-labeled fluorescent secondary antibody diluent (GB25303, Servicebio) was added, and the mixture was incubated for 1 h in the dark. DAPI (4',6-diamidino-2-phenylindole) staining solution was then added, and the mixture was incubated for 10 min in the dark. Images were acquired using a fluorescence microscope, and average fluorescence intensity was analyzed with ImageJ software.

### Animal grouping, modeling, and administration

A total of 48 SPF C57BL/6J mice, aged 8 weeks and weighing ( $20 \pm 2$ ) g, were purchased from Sibefu Biotechnology Co., Ltd. (Beijing, China). The mice were housed in clean feeding cages (ambient temperature 20-24°C, relative humidity 50%-70%, light and dark alternating 12 h each), had free access to food and water, and strictly adhered to the '3R' principle for experimental animals. All animal experimental procedures were approved by the Fourth Affiliated Hospital of China Medical University Ethics Committee.

The mice were adaptively fed for 1 week. They were randomly assigned to the Sham group, the model (bleomycin, BLM) group, the positive control (bleomycin+pirfenidone) group, the orientin low-, medium-, and high-dose (bleomycin+orientin-L, bleomycin+orientin-M, bleomycin+orientin-H) groups, the TGF- $\beta$ 1/Smad3 pathway agonist (bleomycin+orientin+SRI-011381) group, and the inhibitor (bleomycin+orientin+SB431542) group using an interval random grouping method based on body weight, with 6 mice in each group. Except for the Sham group, mice in the other groups were

anesthetized with an intraperitoneal injection of 2% pentobarbital sodium (30 mg/kg) and then secured to the operating table. The mouse pulmonary fibrosis model 4 was prepared by noninvasive tracheal instillation of bleomycin (BLM) (3.75 mg/kg, dissolved in normal saline), and the Sham group received the same volume of normal saline by the same route. After 24 h of modeling, mice in the bleomycin+pirfenidone group were administered 100 mg/kg pirfenidone by gavage. Mice in the low-, medium-, and high-dose groups received 10, 20, and 40 mg/kg of orientin by gavage, respectively. Mice in the SRI-011381 and SB431542 groups were injected intraperitoneally with 30 mg/kg SRI-011381 and 10 mg/kg SB431542, respectively, once daily for 28 days. Two hours after the last administration, the mice were anesthetized and sacrificed, and their lung tissues were dissected.

### Western blot

After HFL1 cells were cultured, RIPA lysis buffer (P0013B, Beyotime) was added to lyse the cells, and the supernatant was collected after centrifugation (4°C, 10 000 r/min, 10 min). Mouse lung tissue was cut into small pieces and placed in a homogenizer tube. Homogenization beads and RIPA lysate were added, and the mixture was lysed on ice for 30 min. The supernatant was collected after centrifugation (4°C, 12 000 r/min, 10 min). The BCA protein concentration assay kit (P0009, Beyotime) was used to determine the total protein concentration in the supernatant. Loading buffer was added, and the protein was denatured in a metal bath at 96°C for 10 min. SDS-PAGE (Sodium Dodecyl Sulfate Polyacrylamide Gel Electrophoresis) was used to separate the protein components (voltage 70-120 V, time 1.5 h). The protein was transferred to a PVDF (polyvinylidene fluoride) membrane by wet transfer (constant current, 300 mA; 2 h), blocked with 5% skimmed milk powder for 2 h, and washed with PBST (phosphate-buffered saline) three times. The primary anti-

bodies were added and incubated overnight at 4°C. The secondary antibody (ab6734, abcam) was added and incubated for 2 h. The chemiluminescence imaging system (Chemi Doc MP, BioRad, USA) was used to expose and capture images, and the gray value of protein bands was analyzed using Image J software.

The primary antibodies: TGF- $\beta$ 1 (81746-2-RR, Proteintech), Smad3 (66516-1-Ig, Proteintech), p-Smad3 (ab63403, Abcam),  $\alpha$ -SMA (67735-1-Ig, Proteintech), fibronectin (ab2413, Abcam), Collagen I (ab316222, Abcam), Vimentin (ab20346, Abcam), matrix metalloproteinase (MMP)-2 (ab181286, Abcam), MMP-9 (ab58803, Abcam), and GAPDH (ab181603, Abcam) were diluted to 1:1,000.

#### **Pathological examination of lung tissue**

The left lung tissues of mice were fixed in 4% paraformaldehyde, dehydrated, cleared, paraffin-embedded, and sectioned (4  $\mu$ m thickness). Hematoxylin and eosin (HE) and Masson staining were performed routinely. Five fields of view were selected for each section. The pathological morphology of lung tissue was observed under an optical microscope, and images were collected. The collagen deposition area in Masson-stained sections was analyzed using ImageJ software.

Lung tissue inflammation scores were assessed according to the Szapiel scoring criteria: 0 score—No alveolar inflammation; 1 score—Monocyte infiltration, widened alveolar septum, limited to local and near-pleural areas, with an area less than 20% of the whole lung, and normal alveolar structure; 2 score—The affected area accounted for 20%-50% of the lung, with the area near the pleura more severe; 3 score—Alveolitis area >50%, with occasional consolidation caused by monocytes and hemorrhage in the alveolar cavity 18.

Pulmonary fibrosis was scored according to the Ashcroft scoring standard: 0 score—normal lung tissue; 1 score—slight thickening of the alveolar or bronchial

walls; 3 score—moderate thickening of the alveolar or bronchial walls, with no obvious damage to the alveolar structure; 5 score—fibrous bands or small fibrous foci were formed, and the alveolar structure was markedly destroyed; 7 score—alveolar structure was severely deformed, and extensive fibrous foci were formed, showing ‘honeycomb lung’; 8 score—full-field fibrosis of lung tissue; the severity of the lesions in the 2, 4, and 6 scores was between the corresponding scores 19.

#### **Bronchoalveolar lavage fluid (BALF) analysis**

After the mice were sacrificed, the chest cavity was opened and the heart removed. The lungs were washed twice with pre-cooled normal saline. The left pulmonary hilum was carefully ligated with a surgical suture, and the trachea was separated at the neck. A V-shaped incision was made at the tracheal bifurcation, and a venous indwelling needle cannula was inserted into the lower bronchus. Then, 500  $\mu$ L of normal saline was slowly injected. Lung swelling was visible to the naked eye, and the lavage fluid was slowly withdrawn. After 3 repeated injections of bronchoalveolar lavage fluid, BALF was collected in a sterile tube, and the supernatant was collected after centrifugation. Tumor necrosis factor-alpha (TNF- $\alpha$ ), interleukin (IL)-2, and IL-6 (ab208348, ab100706, ab222503, Abcam) levels in BALF were measured using enzyme-linked immunosorbent assay (ELISA) kits according to the manufacturer’s instructions. At the same time, the activity of myeloperoxidase (MPO, ab275109, Abcam) in lung tissues was assessed. The total protein content in BALF was measured using a BCA protein concentration assay kit.

#### **Determination of hydroxyproline (HYP) level**

According to the HYP kit (A030-2-1, Jiancheng Institute of Bioengineering, Nanjing, China), 30-100 mg of wet-weight lung

tissue was accurately weighed and placed in a test tube. 1 mL of hydrolysate was added, and the mixture was mixed. The mixture was incubated in a 95°C water bath for 20 min, then diluted with double-distilled water to 10 mL. 4 mL of the diluted hydrolysate was mixed with an appropriate amount of activated carbon, then centrifuged for 10 min. The OD value of each group was measured using 1 mL of supernatant at 550 nm. HYP content in mice was calculated.

### Immunohistochemistry

Lung sections were dewaxed, rehydrated, and antigen-repaired using citrate buffer. Endogenous peroxidase was quenched with 3% H<sub>2</sub>O<sub>2</sub> for 10 min and blocked with 5% BSA for 20 min. Sections were incubated with the  $\alpha$ -SMA antibody (67735-1-Ig, Proteintech, Wuhan, China) overnight at 4°C, then with the secondary antibody solution for 30 min. After washing, DAB (3,3'-diaminobenzidine) staining was performed, and the nuclei were counterstained with hematoxylin.  $\alpha$ -SMA staining was brown, and the sections were evaluated under an optical microscope.

### Statistical analysis

SPSS 27.0 was used for statistical analysis. All data were tested for normality and homogeneity of variance. One-way ANOVA with Tukey's post hoc test was used to compare groups. Data for each group were expressed as mean  $\pm$  standard deviation.  $p < 0.05$  was considered statistically significant.

## RESULTS

### Orientin inhibited TGF- $\beta$ 1-activated HFL1 cell proliferation and migration

TGF- $\beta$ 1 was used to stimulate HFL1 cells to assess the therapeutic effect of orientin on PF, and pirfenidone served as a positive control. The structural formula of orientin is shown in Fig. 1A. First, at concentrations of  $\geq 80 \mu\text{M}$ , the survival rates of HFL1 cells were markedly reduced (Fig. 1B), indicating cellular damage at this con-

centration. Therefore, 10, 20, and 40  $\mu\text{M}$  orientin were selected for subsequent experiments. HFL1 cells were then stimulated with TGF- $\beta$ 1 and treated with pirfenidone and orientin. The proliferation rate of HFL1 cells increased markedly after TGF- $\beta$ 1 stimulation but decreased significantly after pirfenidone and orientin treatment (Fig. 1C). Edu staining showed that Edu-positive cells rose notably after TGF- $\beta$ 1 stimulation and decreased significantly after pirfenidone and orientin treatment (Fig. 1D), indicating that TGF- $\beta$ 1 promoted HFL1 cell proliferation, whereas orientin inhibited this proliferation. TGF- $\beta$ 1 induced the transformation of HFL1 cells into myofibroblasts, and the migration ability of myofibroblasts was enhanced compared with fibroblasts. The migration rate was significantly elevated after TGF- $\beta$ 1 stimulation at 24 h. However, after treatment with pirfenidone and orientin, the migration rate was significantly reduced (Fig. 1E), indicating that orientin suppressed the migratory ability of HFL1 cells. These experiments showed that pirfenidone and orientin significantly suppressed HFL1 cell growth and migration, and the inhibitory effect of high-dose orientin was comparable to that of pirfenidone.

### Orientin inhibited the TGF- $\beta$ 1-activated TGF- $\beta$ 1/Smad3 pathway and inhibited cell proliferation and migration in HFL1 cells

The TGF- $\beta$ 1/Smad3 pathway is a well-characterized pathway implicated in PF progression. This study also found that TGF- $\beta$ 1 and p-Smad3 protein expression in HFL1 cells increased significantly after TGF- $\beta$ 1 induction but decreased significantly after pirfenidone and orientin intervention (Fig. 2A-C), indicating that TGF- $\beta$ 1 induced activation of this pathway, whereas orientin inhibited its activation. Since the inhibitory effect of 40  $\mu\text{M}$  orientin was the most significant in previous studies, this concentration was selected for subsequent research. HFL1 cells were treated with the TGF- $\beta$ 1/Smad3 pathway agonist SRI-011381 and the inhibi-

tor SB431542 alongside orientin treatment. Compared with orientin treatment, TGF- $\beta$ 1 and p-Smad3 protein expression increased significantly after SRI-011381 treatment and decreased significantly after SB431542 treatment (Fig. 2D-F). After SRI-011381 in-

tervention, the proliferation rate of HFL1 cells (Fig. 2G) and Edu-positive cell number (Fig. 2H) increased significantly, and the migration rate also increased significantly (Fig. 2I). SB431542 significantly reduced the proliferation rate, Edu-positive cell num-

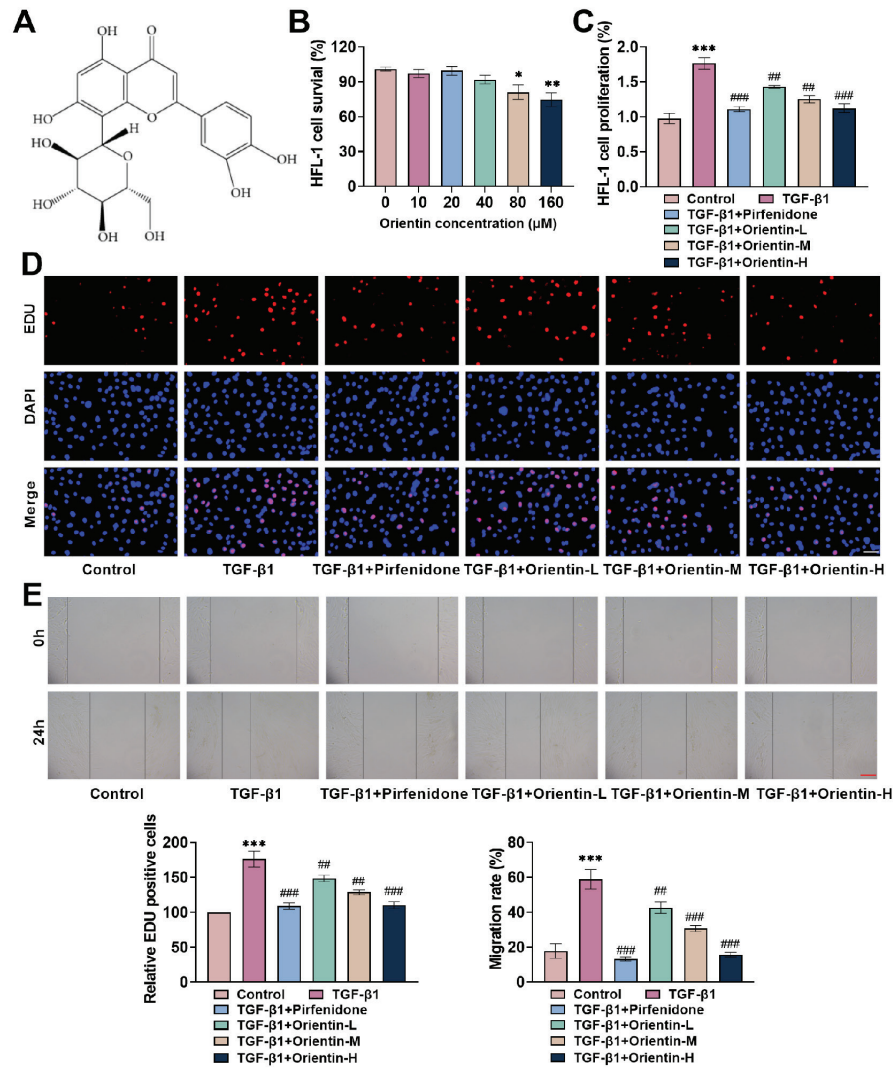


**Fig. 1.** Orientin inhibited TGF- $\beta$ 1-induced HFL1 cell growth and migration. **A:** Orientin molecular formula. **B:** HFL1 (cells derived from human fetal lung tissue) were treated with orientin for 24 h, and the survival rate was measured by CCK-8 assay (Cell Counting Kit-8). Orientin at concentrations of 40  $\mu$ M or lower had no effect on cell viability (\* $p$ <0.05, \*\* $p$ <0.01 vs 0 group). **C:** After HFL1 cells were stimulated with TGF- $\beta$ 1, they were treated with pirfenidone and orientin. The proliferative ability of HFL1 cells was assessed by the CCK-8 assay. Orientin markedly inhibited cell proliferation. **D:** HFL1 cell proliferation was assessed by EdU staining (5-ethynyl-2'-12 deoxyuridine). Orientin decreased the number of EdU-positive cells ( $\times 40$ , 50  $\mu$ m). **E:** The migration of HFL1 cells was assessed by the wound-healing assay. Orientin significantly inhibited cell migration ( $\times 10$ , 200  $\mu$ m). 15  $n$ =3, \* $p$ <0.05, \*\*  $p$ <0.01, \*\*\*  $p$ <0.001 vs 0/Control group; ##  $p$ <0.01, ###  $p$ <0.001 vs TGF- $\beta$ 1 group.

ber, and migration rate of HFL1 cells (Fig. 2G-I), indicating that inhibition of TGF- $\beta$ 1/Smad3 signaling could inhibit HFL1 cell proliferation and migration. In conclusion, ori-

entin suppressed the TGF- $\beta$ 1/Smad3 pathway and inhibited HFL1 cell proliferation and migration.

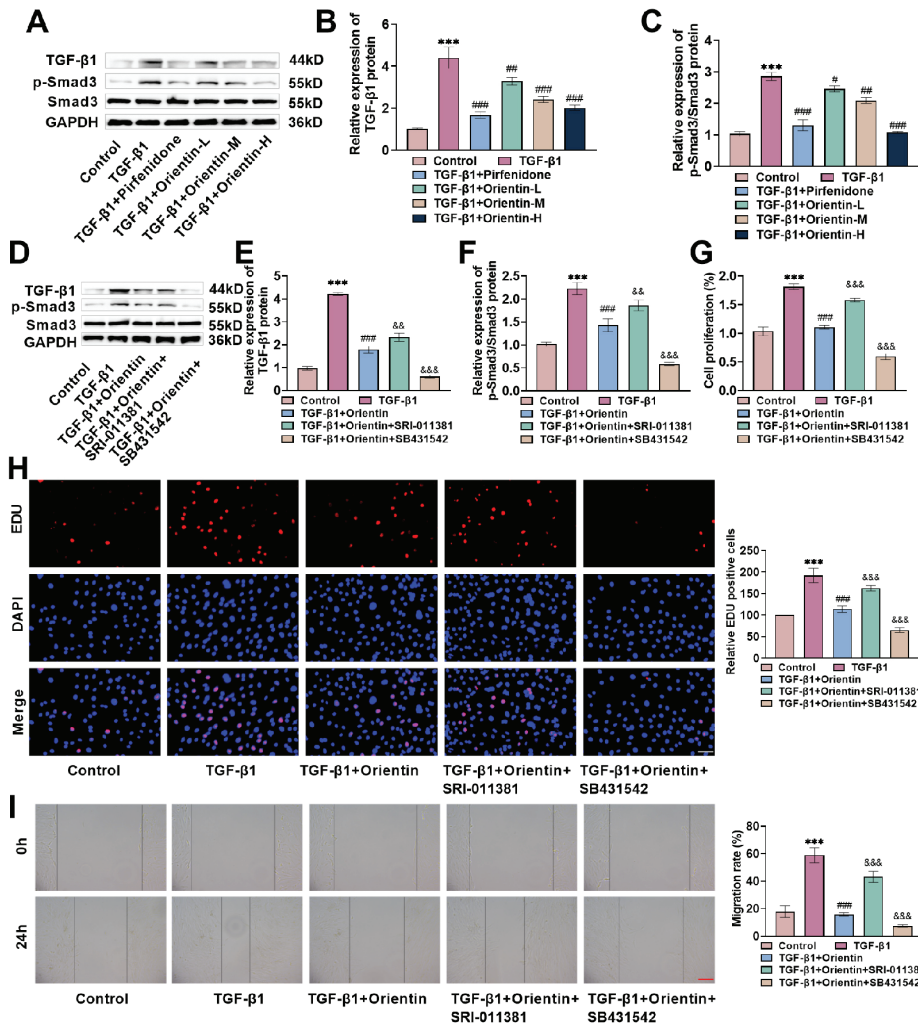


**Fig. 2.** Orientin inhibited TGF- $\beta$ 1-activated TGF- $\beta$ 1/Smad3 pathway and inhibited cell proliferation and migration in HFL1 cells. **A-C:** Western blot was used to detect the expression of the TGF- $\beta$ 1/Smad3 pathway protein in HFL1 cells (cells derived from human fetal lung tissue). Expression of TGF $\beta$ 1 and p-Smad3 protein increased significantly after TGF- $\beta$ 1 induction, and decreased significantly after orientin intervention. **D-F:** HFL1 cells were treated with the TGF $\beta$ 1/Smad3 pathway agonist SRI-011381 (*N*-cyclohexyl-*N*-(phenylmethyl)-*N*-(4-piperidinylmethyl)-urea) and inhibitor SB431542 (TGF- $\beta$  RI Kinase Inhibitor VI) alongside orientin treatment, and TGF- $\beta$ 1/Smad3 pathway protein levels were detected through Western blot. TGF- $\beta$ 1 and p-Smad3 protein expressions increased significantly after SRI-011381 treatment, and decreased significantly after SB431542 treatment. **G:** HFL1 cell proliferation was determined by CCK-8 (Cell Counting Kit-8). SB431542 markedly inhibited cell proliferation. **H:** HFL1 cell proliferation was assessed by EdU staining (5-ethynyl-2'-deoxyuridine). SB431542 significantly reduced the number of EdU-positive cells ( $\times 40$ ,  $50 \mu\text{m}$ ). **I:** Migration was evaluated by the scratch-healing assay. SB431542 significantly inhibited cell migration ( $\times 10$ ,  $200 \mu\text{m}$ ).  $n=3$ , \*\*\*  $p < 0.001$  vs Control group; #  $p < 0.05$ , ##  $p < 0.01$ , ###  $p < 0.001$  vs TGF- $\beta$ 1 group; &  $p < 0.01$ , &&  $p < 0.001$  vs TGF- $\beta$ 1+Orientin group.

### **Orientin inhibited TGF- $\beta$ 1-induced fibroblast to myfibroblast transition (FMT) and improved extracellular matrix (ECM) through the TGF- $\beta$ 1/Smad3 signaling pathway**

Fibroblasts are primarily responsible for producing and maintaining the ECM, and their mechanical properties can be altered. They can also transform into myofibroblasts. Myofibroblasts are cells that drive fibrotic tissue development through a sharp increase in protein deposition. The transition from fibroblasts to myofibroblasts is a well-known cellular marker of histopathological status<sup>20</sup>. Sirius red staining showed that collagen fiber staining increased significantly after TGF- $\beta$ 1 stimulation and decreased significantly after orientin treatment. However, compared with orientin treatment, red-stained collagen fibers increased significantly after SRI-011381 treatment and decreased significantly after SB431542 treatment (Fig. 3A), indicating that orientin inhibited the production and accumulation of collagen fibers induced by TGF- $\beta$ 1 through the TGF- $\beta$ 1/Smad3 pathway.  $\alpha$ -SMA is a marker of myofibroblasts. The fluorescence intensity of  $\alpha$ -SMA increased significantly after TGF- $\beta$ 1 intervention, decreased significantly after orientin treatment, increased significantly after SRI-011381 treatment, and decreased significantly after SB431542 treatment (Fig. 3B). Finally, ECM-related protein expression was assessed by Western blot.  $\alpha$ -SMA, fibronectin, Collagen I, Vimentin, MMP-2, and MMP-9 protein levels were markedly elevated after TGF- $\beta$ 1 stimulation but declined markedly after orientin treatment. Compared with orientin intervention, protein levels were significantly increased after SRI-011381 treatment and significantly decreased after SB431542 treatment (Fig. 3C-I), indicating that orientin improved ECM through the TGF- $\beta$ 1/Smad3 pathway. Overall, these experiments showed that orientin inhibited TGF- $\beta$ 1-induced FMT, reduced ECM deposition, and promoted ECM remodeling by suppressing the TGF- $\beta$ 1/Smad3 pathway.

### **Orientin inhibited the BLM-activated TGF- $\beta$ 1/Smad3 pathway in mouse lung tissue**

To further verify the protective effects of orientin in vivo, this study established a BLM-induced PF mouse model to verify the in vivo mechanism and treated the mice with pirfenidone and orientin. TGF- $\beta$ 1 and p-Smad3 protein expression increased markedly after BLM induction but decreased significantly after pirfenidone and orientin treatment, with the high-dose orientin intervention effect comparable to that of pirfenidone (Fig. 4A-C). However, after injection of SRI-011381, TGF- $\beta$ 1 and p-Smad3 levels were notably raised. The protein levels were significantly reduced after injection of SB431542 (Fig. 4D-F). This indicated that orientin suppressed the BLM-induced TGF- $\beta$ 1/Smad3 pathway.

### **Orientin alleviated BLM-induced inflammatory injury in mouse lung tissue by the TGF- $\beta$ 1/Smad3 pathway**

HE staining showed that the lung tissue structure in the bleomycin group was destroyed, with alveolar cavities collapsed, alveolar septa widened, and inflammatory infiltration within the alveolar cavities. The inflammatory score of the lung tissue increased significantly. After orientin treatment, inflammatory infiltration and the score were significantly reduced. After SRI-011381 treatment, the alveolar space in lung tissue decreased, inflammatory infiltration increased, and the score increased. Lung tissue inflammation was inhibited after SB431542 treatment (Fig. 5A). TNF- $\alpha$ , IL-2, and IL-6 levels in BALF, and MPO (myeloperoxidase) activity in lung tissue, increased significantly after BLM stimulation and decreased significantly after orientin treatment. Compared with orientin treatment, inflammatory factors and MPO levels were significantly increased after SRI-011381 treatment and significantly decreased after SB431542 treatment (Fig. 5B-E). The trend of total protein content in BALF was consis-

tent with that of inflammatory factors, increasing significantly after treatment with BLM and SRI-011381, and decreasing significantly after treatment with orientin and

SB431542 (Fig.5F). In summary, orientin can alleviate the degree of inflammation in PF mice by suppressing the TGF- $\beta$ 1/Smad3 pathway.

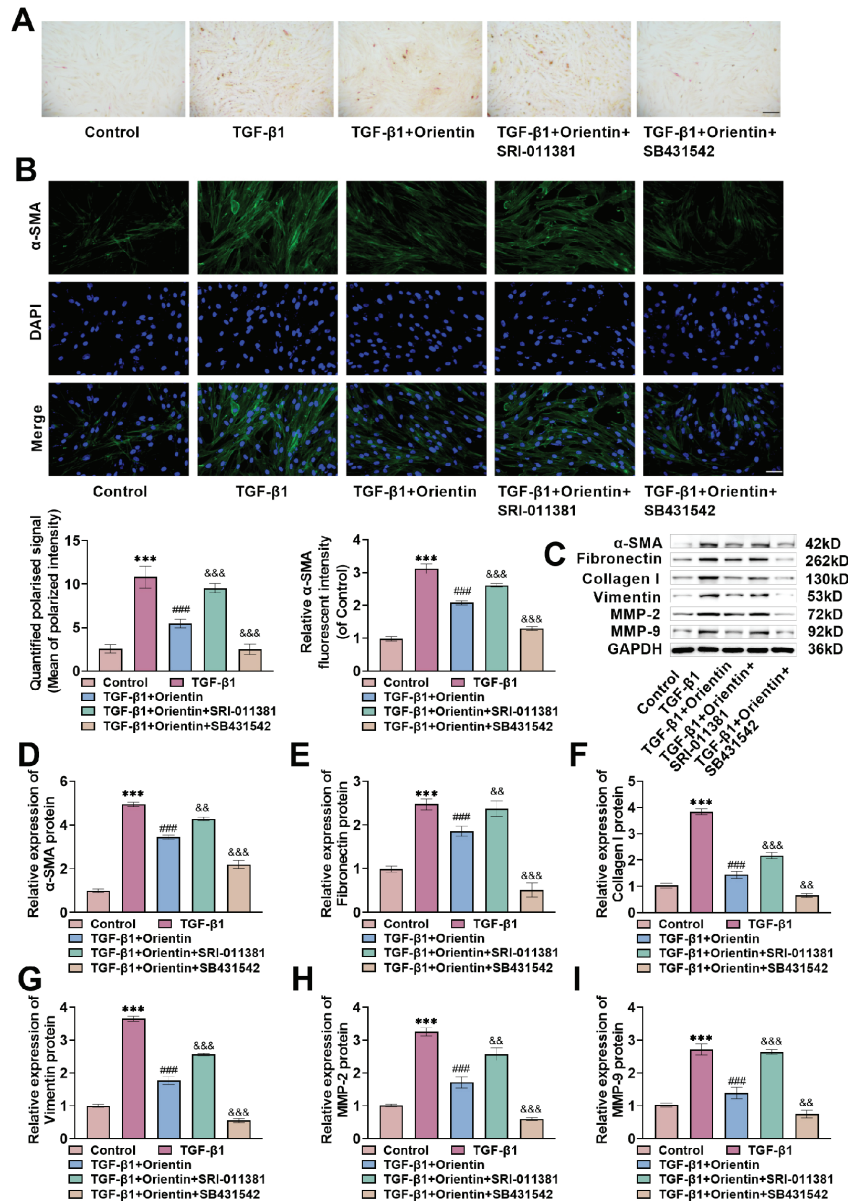


**Fig. 3.** Orientin inhibited TGF- $\beta$ 1-induced FMT and improved ECM by TGF $\beta$ 1/Smad3 pathway. **A:** Sirius red staining was used to detect the type of cell collagen fibers. Red-stained collagen fibers were significantly reduced after Orientin treatment ( $\times 20$ ,  $100 \mu\text{m}$ ). **B:**  $\alpha$ -SMA levels were assessed by immunofluorescence. Orientin significantly reduced  $\alpha$ -SMA fluorescence intensity ( $\times 40$ ,  $50 \mu\text{m}$ ). **C-I:** ECM (extracellular matrix)-related protein expression was determined by Western blot.  $\alpha$ -SMA, fibronectin, Collagen I, Vimentin, MMP-2 (matrix metalloproteinase-2), and MMP-9 (matrix metalloproteinase-9) levels were markedly decreased after Orientin therapy.  $n=3$ , \*\*\*  $p<0.001$  vs Control group; ###  $p<0.001$  vs TGF- $\beta$ 1 group; &&  $p<0.01$ , &&&  $p<0.001$  vs TGF- $\beta$ 1+Orientin group. TGF- $\beta$ 1.

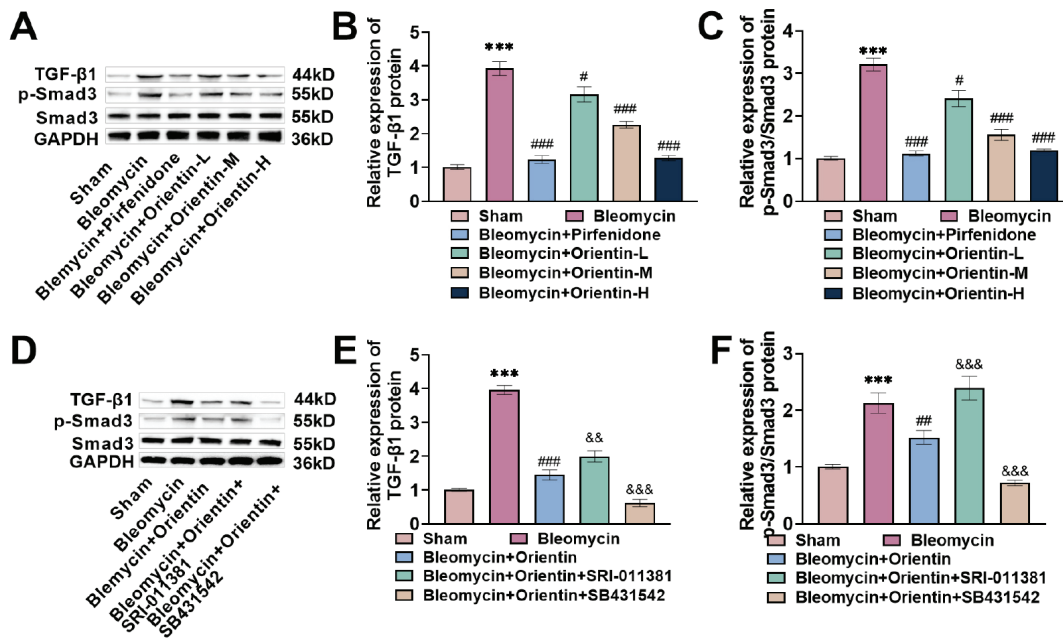


**Fig. 4.** Orientin inhibited BLM-induced activation of the TGF- $\beta$ 1/Smad3 pathway in mouse lung tissue. **A-C:** Protein expression of the TGF- $\beta$ 1/Smad3 pathway was evaluated by Western blot. TGF- $\beta$ 1 and p-Smad3 protein (phosphorylated SMAD family member 3) levels were markedly increased after BLM induction, and significantly lowered after orientin intervention. **D-F:** The mice were injected with the TGF- $\beta$ 1/Smad3 pathway agonist SRI-011381 (*N'*-cyclohexyl-*N*-(phenylmethyl)-*N*-(4-piperidinylmethyl)-urea) and the inhibitor SB431542 (TGF- $\beta$  RI Kinase Inhibitor VI) at the same time as orientin, and TGF- $\beta$ 1/Smad3 pathway protein levels were determined by Western blot. p-Smad3 (phosphorylated SMAD family member 3) and TGF- $\beta$ 1 levels were significantly increased when SRI-011381 intervention, and significantly decreased after SB431542 treatment.  $n=6$ ,  $***p<0.001$  vs sham group; #  $p<0.05$ , ##  $p<0.01$ , ###  $p<0.001$  vs treatment.  $n=6$ ,  $***p<0.001$  vs sham group; #  $p<0.05$ , ##  $p<0.01$ , ###  $p<0.001$  vs.

### Orientin alleviated BLM-induced PF injury in mice through the TGF- $\beta$ 1/Smad3 pathway

HYP content in lung tissue increased significantly after BLM stimulation and decreased significantly after orientin treatment. Compared with orientin treatment, HYP content increased significantly after SRI-011381 treatment and decreased significantly after SB431542 treatment (Fig. 6A). Masson staining showed that the structure of lung tissue in the bleomycin group was destroyed, collagen fibers were severely proliferated, and the collagen deposition area and pulmonary fibrosis score were significantly increased. After orientin treatment, the degree of alveolar damage and

collagen fiber hyperplasia were significantly reduced, and the collagen deposition area and pulmonary fibrosis score were significantly reduced. After the SRI-011381 intervention, collagen fiber proliferation was notably elevated, and the collagen deposition area and PF score were markedly increased. After SB431542 treatment, collagen fiber proliferation was reduced, and the collagen deposition area and PF score were notably reduced (Fig.6B-D).  $\alpha$ -SMA levels were consistent with those in cell experiments, being markedly raised after BLM and SRI-011381 treatment and significantly decreased after orientin and SB431542 treatment (Fig. 6E). Fibronectin, Collagen I,  $\alpha$ -SMA, Vimentin, MMP-2, and MMP-9 expressions increased

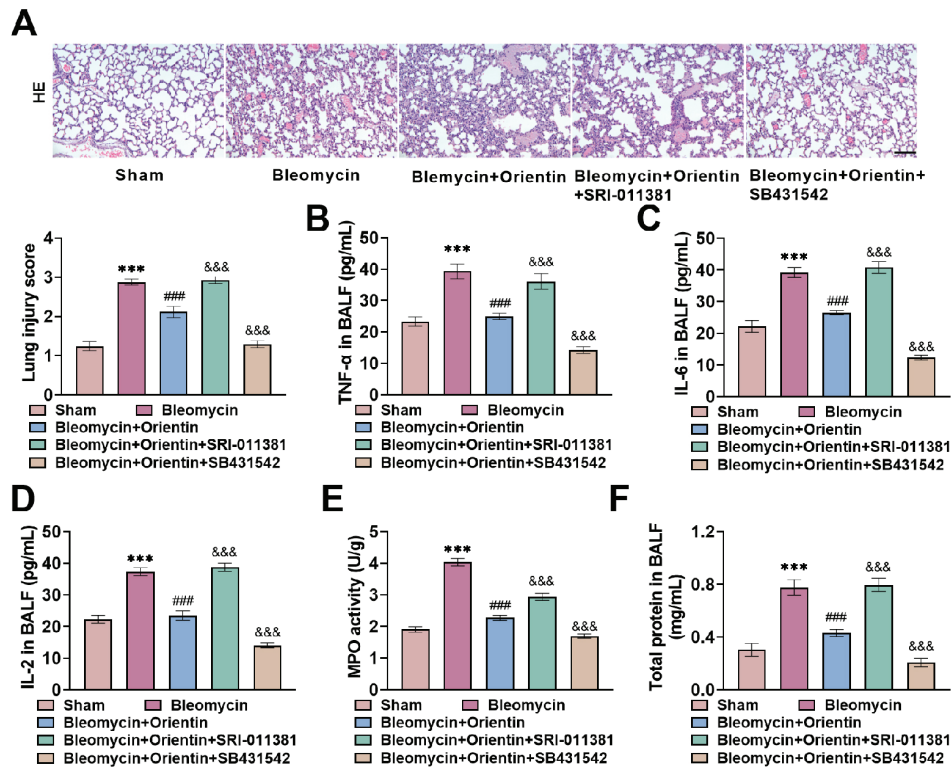


**Fig. 5.** Orientin alleviated BLM-induced inflammatory injury in mouse lung tissue via the TGF- $\beta$ 1/Smad3 pathway. **A:** Pathological damage to lung tissue in each group was observed by HE staining. After BLM stimulation, alveolar cavity collapse, inflammatory cell infiltration, and inflammatory score increased significantly. Orientin can inhibit lung inflammation ( $\times 20$ ,  $100 \mu\text{m}$ ). **B-E:** TNF- $\alpha$ , IL-2 and IL-6 levels in BALF and MPO activity in lung tissues were determined using an ELISA kit. These were significantly reduced after Orientin treatment. **F:** The total protein content in BALF was determined by the BCA (bicinchoninic acid) method, which was significantly decreased after Orientin treatment.  $n=6$ , \*\*\*  $p<0.001$  vs sham group; ###  $p<0.001$  vs the bleomycin group; &&&  $p<0.001$  vs the bleomycin+orientin group. SRI-011381 ( $N'$ -cyclohexyl- $N$ -(phenylmethyl)- $N$ -(4-piperidinylmethyl)-urea); SB431542 (TGF- $\beta$  RI Kinase Inhibitor VI).

markedly after BLM stimulation but decreased significantly after orientin treatment. Compared with orientin intervention, protein levels were significantly increased after SRI-011381 treatment and significantly decreased after SB431542 treatment (Fig. 6F-L). These experiments showed that orientin could alleviate fibrosis damage in PF mice by suppressing the TGF- $\beta$ 1/Smad3 pathway.

## DISCUSSION

This study was the first to systematically evaluate the therapeutic effect of orientin

on PF and its underlying molecular mechanism. Orientin notably reduced pathological changes in lung tissue, inhibited FMT, improved ECM, and lessened the severity of PF. The mechanism was closely associated with reducing the inflammatory response and inhibiting the TGF- $\beta$ 1/Smad3 pathway.

Myofibroblasts are absent from normal lung tissue but are important producers of collagen and other matrix proteins. Promoting fibroblast apoptosis and inhibiting fibroblast-to-myofibroblast transformation can effectively inhibit PF<sup>21</sup>. TGF- $\beta$ 1, a key cytokine that promotes myofibroblast

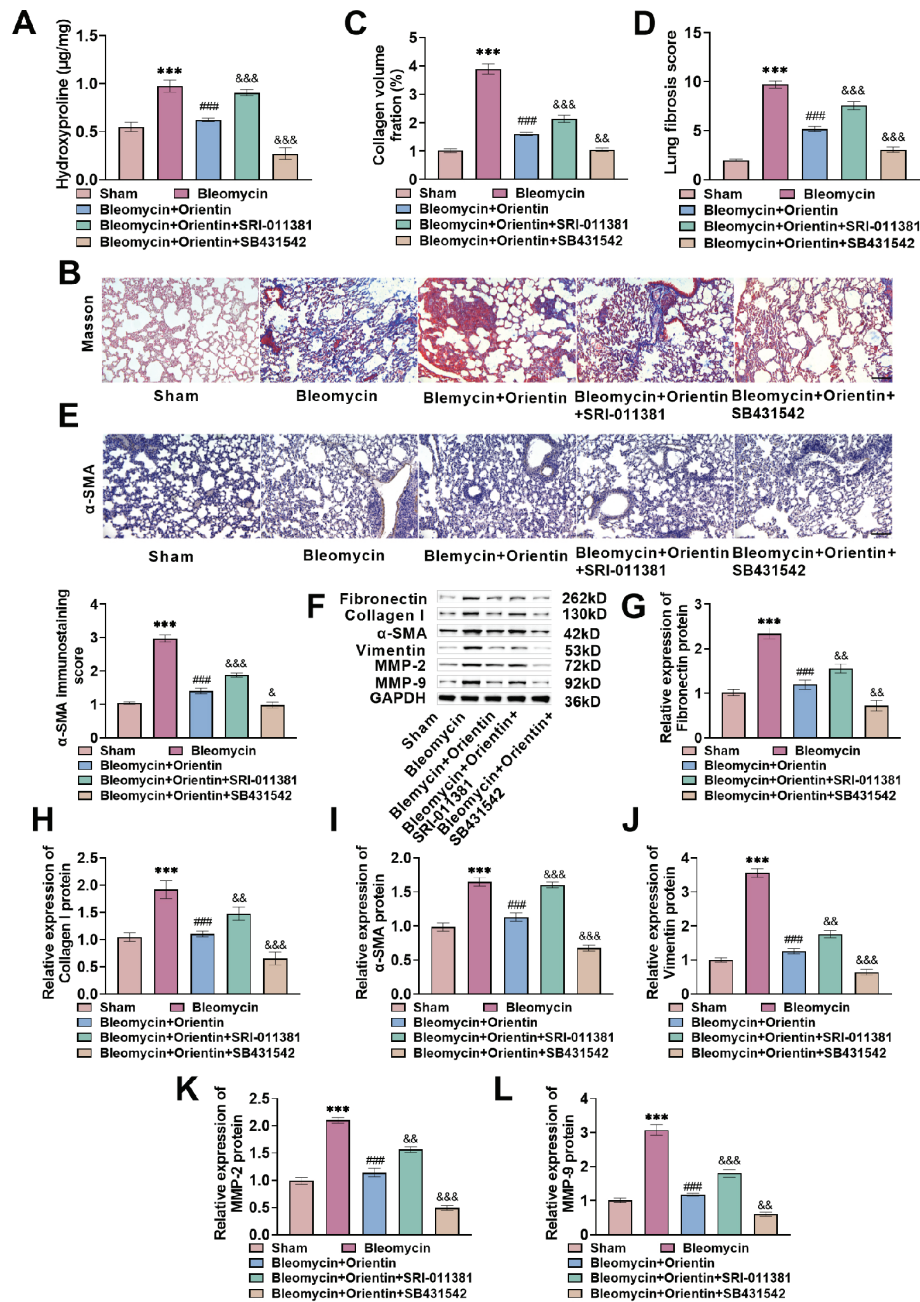


**Fig. 6.** Orientin alleviated BLM-induced PF injury in mice through the TGF- $\beta$ 1/Smad3 pathway. **A:** HYP content in lung tissue was measured by HYP assay, and was significantly reduced after orientin treatment. **B-D:** Collagen deposition and fibrosis were analyzed by Masson-Brüch staining. After BLM stimulation, collagen fibers in lung tissue proliferated significantly, and the collagen deposition area and PF score increased significantly. The collagen deposition area and pulmonary fibrosis score were markedly reduced after orientin therapy ( $\times 20$ ,  $100 \mu\text{m}$ ). **E:**  $\alpha$ -SMA level was evaluated by immunohistochemistry. Orientin significantly reduced  $\alpha$ -SMA level ( $\times 20$ ,  $100 \mu\text{m}$ ). **F-L:** PF-related protein levels were detected by Western blot. The levels of  $\alpha$ -SMA, fibronectin, Collagen I, Vimentin, MMP-2, and MMP-9 were markedly decreased after Orientin intervention.  $n=6$ , \*\*\*  $p<0.001$  vs the sham group; ###  $p<0.001$  vs the bleomycin group; &  $p<0.05$ , &&  $p<0.01$ , &&&  $p<0.001$  vs the bleomycin+orientin group. SRI-011381 (N'-cyclohexyl-N-(phenylmethyl)-N-(4-piperidinylmethyl)-urea); SB431542 (TGF- $\beta$  RI Kinase Inhibitor VI).

differentiation and collagen expression, is vital for the progression of PF. As our understanding of PF pathogenesis advances, TGF- $\beta$ 1 has been identified as the primary pro-fibrotic growth factor involved in fibrosis, influencing cell growth, differentiation, and programmed cell death. Excess TGF- $\beta$ 1 results in collagen accumulation and triggers various fibrotic conditions<sup>22</sup>. Therefore, this study used TGF- $\beta$ 1 to induce fibroblasts and construct an in vitro PF model. The results showed that orientin significantly suppressed TGF- $\beta$ 1-activated proliferation and migration of HEL1 cells.

In this study, the anti-fibrosis mechanism of orientin was further elucidated by systematically evaluating changes in key indicators of the TGF- $\beta$ 1/Smad3 pathway. At the ligand level, TGF- $\beta$ 1 is the central factor that initiates and maintains fibrosis, and its activity directly determines the severity of fibrosis<sup>23</sup>. At the level of intracellular signal transduction, the phosphorylation level of Smad3 is a direct indicator of TGF- $\beta$ 1 pathway activity<sup>24</sup>. At the effector-molecule level,  $\alpha$ -SMA is a specific marker of fibroblast activation; its expression directly reflects the activation state of fibroblasts. At the same time, ECM remodeling is an important factor in promoting the occurrence and development of PF. Intervention in ECM remodeling can significantly improve excessive fibrosis in the lung<sup>25, 26</sup>. Collagen I and fibronectin are major ECM components; their high expression can lead to pulmonary interstitial collagen deposition<sup>27, 28</sup>. MMPs are collagenolytic enzymes that are vital to the pathophysiological process of IPF. High expression of MMPs degrades the basement membrane and lung tissue structure, collapses the alveolar cavity, aggravates lung injury, and further promotes the release of TGF- $\beta$ 1. TGF- $\beta$ 1, as an activator of MMPs, promotes their synthesis and further increases MMP expression, thus forming a vicious circle<sup>29</sup>.

This study found that orientin significantly reduced TGF- $\beta$ 1 and p-Smad3 levels

in HEL1 cells after TGF- $\beta$ 1 stimulation, indicating that orientin inhibited the TGF- $\beta$ 1/Smad3 pathway and that this inhibition also suppressed HEL1 cell proliferation and migration. In addition, TGF- $\beta$ 1 significantly increased collagen fiber formation in HEL1 cells and upregulated  $\alpha$ -SMA, fibronectin, Collagen I, Vimentin, and MMP expression, suggesting that TGF- $\beta$ 1 notably promoted lung fibroblast activation, FMT, and excessive ECM deposition. Orientin could inhibit the TGF- $\beta$ 1/Smad3 pathway, thereby inhibiting lung fibroblast activation, improving ECM, and alleviating the PF process. ECM and collagen deposition are the key pathological changes that cause PF, indicating that Orientin improved these key pathological changes.

PF involves a series of inflammatory and fibrotic reactions that ultimately lead to ECM deposition, fibroblast foci, and fibrotic areas juxtaposed with normal lung parenchyma. In the early stage of IPF, the balance of M1/M2 macrophages is disrupted, leading to the secretion of inflammatory mediators and the recruitment of fibroblasts, which proliferate continuously. TNF- $\alpha$ , IL-1 $\beta$ , IL-6, and IL-2 are key biomarkers for assessing the inflammatory state of lung tissue. They jointly promote inflammatory injury and fibrosis in lung tissue by recruiting, activating, and expanding inflammatory cells, and by regulating the immune response and tissue repair processes in the development of PF<sup>3</sup>. Studies have shown that orientin can reduce LPS-induced NF- $\kappa$ B phosphorylation in cells, thereby lowering inflammatory factors and oxidative markers<sup>17</sup>. MPO activity is a marker of neutrophil infiltration in lung tissue<sup>30</sup>. Neutrophils release numerous toxic substances during inflammation, causing damage to the lung parenchyma and tissue structure. Neutrophils are key inflammatory cells that drive PF<sup>31, 32</sup>. The most commonly used and well-established drug for inducing lung fibrosis in rats is BLM<sup>33</sup>. In this study, lung tissues after BLM intervention were significantly damaged, with alveo-

lar collapse, atrophy, widened intervals, and inflammatory cell infiltration. In addition, a large number of inflammatory cytokines accumulated in BALF after BLM induction, and MPO activity in lung tissues was markedly elevated. However, inflammatory infiltration in the pirfenidone and orientin groups was significantly reduced, and the levels of TNF- $\alpha$ , IL-2, IL-6, and MPO activity were also significantly reduced. SRI-011381 significantly weakened orientin's anti-inflammatory effects, whereas SB431542 significantly enhanced them. This suggests that orientin may reduce the release of inflammatory factors and inflammatory infiltration via the TGF- $\beta$ 1/Smad3 axis, thereby slowing the PF process.

After modeling with BLM, the initial damage was primarily concentrated around the bronchioles; on the 7th day, the distal lung parenchyma was involved, and multiple inflammatory lesions and edema were observed in the alveolar septa. On the 14th day, regional interstitial fibrosis appeared in the lungs, manifested as extensive collagen deposition and remodeling of alveolar units. These changes are considered to reflect similar changes in PF. Based on this, the model can complete the task of studying PF mitigation drugs. HYP is a unique amino acid in collagen and is one of the main components of collagen tissue. Some data confirmed that HYP can be used as a reliable method for quantitative fibrosis<sup>4</sup>. In the BLM-induced PF rat model, this study, using Masson staining, observed that collagen fibers after BLM intervention were markedly proliferated, the collagen deposition area and PF score were markedly increased, and the HYP content was significantly increased. Collagen deposition

in the pirfenidone and orientin groups was notably reduced, and the PF score and HYP content were significantly reduced, indicating that orientin and pirfenidone can effectively alleviate BLM-induced pulmonary fibrosis. Western blot experiments also confirmed that the expressions of fibronectin, Collagen I,  $\alpha$ -SMA, Vimentin, MMP-2, and MMP-9 were significantly decreased after orientin treatment. However, SRI-011381 significantly weakened orientin's anti-fibrosis effect, whereas SB431542 significantly enhanced it. Therefore, orientin can inhibit lung fibroblast activation and reduce collagen deposition in the lungs of PF mice via the TGF- $\beta$ 1/Smad3 pathway. Combined with the results of cell experiments, Orientin can inhibit FMT through the TGF- $\beta$ 1/Smad3 pathway, alleviate inflammatory responses and fibrotic damage, and thereby improve PF, indicating the potential of Orientin as a therapeutic drug for PF.

In summary, orientin can inhibit inflammatory factors and FMT in a PF model, reduce ECM production, regulate key protein expression in the TGF- $\beta$ 1/Smad3 pathway, and demonstrate a clear anti-fibrotic effect. As a natural medicine with a wide range of sources and low cost, orientin has promising applications in PF treatment. This study provides laboratory evidence supporting the use of orientin as a therapeutic agent for PF. Follow-up studies can further explore its clinical translational value and provide new treatment options for PF patients. Although this study reveals the potential role of orientin in PF and its molecular mechanism, differences between rodents and humans introduce uncertainty in translating the results, which can be further explored and verified using PF patient samples.

### List of abbreviations

TGF-β1	transforming growth factor-β1
Smad3	suppressor of mother against decapentaplegic 3
HYP	hydroxyproline
FMT	fibroblast to myofibroblast transition
PF	pulmonary fibrosis
IPF	idiopathic pulmonary fibrosis
ECM	extracellular matrix
EMT	epithelial-mesenchymal transition
α-SMA	alpha-smooth muscle actin
MMP	matrix metalloproteinase
BALF	bronchoalveolar lavage fluid
TNF-α	tumour necrosis factor-alpha
IL	interleukin
MPO	myeloperoxidase
IMP	Imperatorin
BLM	bleomycin

### Acknowledgment

None.

### Funding

None.

### ORCID ID of the authors

- Yijin Liu (YiL):  
0009-0000-9374-5973
- Yao Lu (YaL):  
0009-0007-2749-1419

### Author's contributions

YaL: Developed and planned the study, performed experiments, and interpreted results. Edited and refined the manuscript with a focus on critical intellectual contributions. YaL: Participated in collecting, assessing, and interpreting the data. Made significant contributions to data interpretation and manuscript preparation. Yi L: Provided substantial intellectual input during the drafting and revision of the manuscript.

### Conflict of interest

The authors state that they have no conflicts of interest.

### Consent to publish

The manuscript has neither been previously published nor is under consideration by any other journal. The authors have all approved the content of the paper.

### Ethic approval

This study was approved by The Fourth Affiliated Hospital of China Medical University Ethic Committee (No. 21000062024112).

### REFERENCES

1. Kawano-Dourado L, Funke-Chambour M, Wells AU. Ziritaxestat and Lung Function in Idiopathic Pulmonary Fibrosis. *JAMA*. 2023;330(10):973. <https://doi.org/10.1001/jama.2023.12637>.
2. Savin IA, Zenkova MA, Sen'kova AV. Pulmonary Fibrosis as a Result of Acute Lung Inflammation: Molecular Mechanisms, Relevant In Vivo Models, Prognostic and Therapeutic Approaches. *Int J Mol Sci*. 2022;23(23):14959. <https://doi.org/10.3390/ijms232314959>.
3. Liu GY, Budinger GRS, Dematte JE. Advances in the management of idiopathic pulmonary fibrosis and progressive pulmonary fibrosis. *BMJ*. 2022;377:e066354. <https://doi.org/10.1136/bmj-2021-066354>.
4. Zhang Y, Lu YB, Zhu WJ, Gong XX, Qian R, Lu YJ, et al. Leech extract alleviates idiopathic pulmonary fibrosis by TGF-β1/Smad3 signaling pathway. *J Ethnopharmacol*. 2024;324:117737. <https://doi.org/10.1016/j.jep.2024.117737>.
5. Yao F, Xu M, Dong L, Shen X, Shen Y, Jiang Y, et al. Sinomenine attenuates pulmonary fibrosis by downregulating TGF-β1/Smad3, PI3K/Akt and NF-κB signaling pathways. *BMC Pulm Med*. 2024;24(1):229. <https://doi.org/10.1186/s12890-024-03050-5>.

6. Yang F, Hou ZF, Zhu HY, Chen XX, Li WY, Cao RS, et al. Catalpol Protects Against Pulmonary Fibrosis Through Inhibiting TGF- $\beta$ 1/Smad3 and Wnt/ $\beta$ -Catenin Signaling Pathways. *Front Pharmacol*. 2021;11:594139. <https://doi.org/10.3389/fphar.2020.594139>.
7. Wanas H, El Shereef Z, Rashed L, Aboulhoda BE. Ticagrelor Ameliorates Bleomycin-Induced Pulmonary Fibrosis in Rats by the Inhibition of TGF- $\beta$ 1/Smad3 and PI3K/AKT/mTOR Pathways. *Curr Mol Pharmacol*. 2022;15(1):227-238. <https://doi.org/10.2174/1874467214666210204212533>.
8. Truchetet ME, Brembilla NC, Chizzolini C. Current Concepts on the Pathogenesis of Systemic Sclerosis. *Clin Rev Allergy Immunol*. 2023;64(3):262-283. <https://doi.org/10.1007/s12016-021-08889-8>.
9. Moss BJ, Ryter SW, Rosas IO. Pathogenic Mechanisms Underlying Idiopathic Pulmonary Fibrosis. *Annu Rev Pathol*. 2021;17:515-546. <https://doi.org/10.1146/annurev-pathol-042320-030240>
10. Wang J, Xu L, Xiang Z, Ren Y, Zheng X, Zhao Q, et al. Microcystin-LR ameliorates pulmonary fibrosis via modulating CD206(+) M2-like macrophage polarization. *Cell Death Dis*. 2020;11(2):136. <https://doi.org/10.1038/s41419-020-2329-z>.
11. Zhu D, Zhang Q, Li Q, Wang G, Guo Z. Inhibition of AHNK nucleoprotein 2 alleviates pulmonary fibrosis by downregulating the TGF- $\beta$ 1/Smad3 signaling pathway. *J Gene Med*. 2022;24(9):e3442. <https://doi.org/10.1002/jgm.3442>.
12. Liu H, Lai W, Nie H, Shi Y, Zhu L, Yang L, et al. PM(2.5) triggers autophagic degradation of Caveolin-1 via endoplasmic reticulum stress (ERS) to enhance the TGF- $\beta$ 1/Smad3 axis promoting pulmonary fibrosis. *Environ Int*. 2023;181:108290. <https://doi.org/10.1016/j.envint.2023.108290>.
13. Ghafouri-Fard S, Askari A, Shoorei H, Seify M, Koohestanidehaghi Y, Hussien BM, et al. Antioxidant therapy against TGF- $\beta$ /SMAD pathway involved in organ fibrosis. *J Cell Mol Med*. 2024;28(2):e18052. <https://doi.org/10.1111/jcmm.18052>.
14. Fahmy MI, Sadek MA, Abdou K, El-Dessouki AM, El-Shiekh RA, Khalaf SS. Orientin: a comprehensive review of a promising bioactive flavonoid. *Inflammopharmacology*. 2025;33(4):1713-1728. <https://doi.org/10.1007/s10787-025-01690-5>.
15. Long Q, Ma T, Wang Y, Chen S, Tang S, Wang T, et al. Orientin alleviates the inflammatory response in psoriasis like dermatitis in BALB/c mice by inhibiting the MAPK signaling pathway. *Int Immunopharmacol*. 2024;134:112261. <https://doi.org/10.1016/j.intimp.2024.112261>.
16. Chen H, Liu S, Xing J, Wen Y, Chen L. Orientin alleviates chondrocyte senescence and osteoarthritis by inhibiting PI3K/AKT pathway. *Bone Joint Res*. 2025;14(3):245-258. *Bone Joint Res*. 2025 Mar 14;14(3):245-258. <https://doi.org/10.1302/2046-3758.143.BJR-2023-0383.R2>.
17. Xiao Q, Cui Y, Zhao Y, Liu L, Wang H, Yang L. Orientin relieves lipopolysaccharide-induced acute lung injury in mice: The involvement of its anti-inflammatory and anti-oxidant properties. *Int Immunopharmacol*. 2021;90:107189. <https://doi.org/10.1016/j.intimp.2020.107189>.
18. Szapiel SV, Elson NA, Fulmer JD, Hunnigake GW, Crystal RG. Bleomycin-induced interstitial pulmonary disease in the nude, athymic mouse. *Am Rev Respir Dis*. 1979;120(4):893-899. <https://doi.org/10.1164/arrd.1979.120.4.893>.
19. Ashcroft T, Simpson JM, Timbrell V. Simple method of estimating severity of pulmonary fibrosis on a numerical scale. *J Clin Pathol*. 1988;41(4):467-470. <https://doi.org/10.1136/jcp.41.4.467>.
20. D'Urso M, Kurniawan NA. Mechanical and Physical Regulation of Fibroblast-Myofibroblast Transition: From Cellular Mechanoresponse to Tissue Pathology. *Front Bioeng Biotechnol*. 2020;8:609653. <https://doi.org/10.3389/fbioe.2020.609653>.
21. Zhang JX, Huang PJ, Wang DP, Yang WY, Lu J, Zhu Y, et al. m(6)A modification regulates lung fibroblast-to-myofibroblast transition through modulating KCNH6 mRNA translation. *Mol Ther*.

- 2021;29(12):3436-3448. <https://doi.org/10.1016/j.ymthe.2021.06.008>.
22. **Gifford CC, Tang J, Costello A, Khakoo NS, Nguyen TQ, Goldschmeding R, et al.** Negative regulators of TGF- $\beta$ 1 signaling in renal fibrosis; pathological mechanisms and novel therapeutic opportunities. *Clin Sci*. 2021;135(2):275-303. <https://doi.org/10.1042/CS20201213>.
23. **Glass DS, Grossfeld D, Renna HA, Agarwala P, Spiegler P, Kasselmann LJ, et al.** Idiopathic pulmonary fibrosis: Molecular mechanisms and potential treatment approaches. *Respir Investig*. 2020;58(5):320-335. <https://doi.org/10.1016/j.resinv.2020.04.002>.
24. **Ye Z, Hu Y.** TGF- $\beta$ 1: Gentlemanly orchestrator in idiopathic pulmonary fibrosis (Review). *Int J Mol Med*. 2021;48(1):132. <https://doi.org/10.3892/ijmm.2021.4965>.
25. **Ding H, Cui Y, Yang J, Li Y, Zhang H, Ju S, et al.** ROS-responsive microneedles loaded with integrin  $\alpha$ v $\beta$ 6-blocking antibodies for the treatment of pulmonary fibrosis. *J Control Release*. 2023;360:365-375. <https://doi.org/10.1016/j.jconrel.2023.03.060>.
26. **Habert P, Puech B, Coiffard B, Secq V, Thomas P, Bec R, et al.** Angiographic and histopathological study on bronchial-to-pulmonary vascular anastomoses on explants from patients with cystic fibrosis after bronchial artery embolisation. *J Cyst Fibros*. 2022;21(6):1042-1047. <https://doi.org/10.1016/j.jcf.2022.04.015>.
27. **Patten J, Wang K.** Fibronectin in development and wound healing. *Adv Drug Deliv Rev*. 2021;170:353-368. <https://doi.org/10.1016/j.addr.2020.09.005>.
28. **Yan Y, Zhang Y, Zhang J, Ying L.** SCN-N1B regulates the proliferation, migration, and collagen deposition of human lung fibroblasts. *In Vitro Cell Dev Biol Anim*. 2023;59(7):479-485. <https://doi.org/10.1007/s11626-023-00787-x>.
29. **Mahalanobish S, Saha S, Dutta S, Sil PC.** Matrix metalloproteinase: An upcoming therapeutic approach for idiopathic pulmonary fibrosis. *Pharmacol Res*. 2020;152:104591. <https://doi.org/10.1016/j.phrs.2019.104591>.
30. **Xin Y, Zou L, Lang S.** 4-Octyl itaconate (4-OD) attenuates lipopolysaccharide-induced acute lung injury by suppressing PI3K/Akt/NF- $\kappa$ B signaling pathways in mice. *Exp Ther Med*. 2021;21(2):141. <https://doi.org/10.3892/etm.2020.9573>.
31. **Chen S, Song X, Lv C.** Macrophages and Pulmonary Fibrosis. *Curr Mol Med*. 2025;25(4):416-430. <https://doi.org/10.2174/0115665240286046240112112310>.
32. **Ay D, Başlılar Ş, Kulah G, Kaan Saylan B, Kalbaran Kismet G, Okutan O.** Blood Cell Counts and Inflammatory Indexes in Idiopathic Pulmonary Fibrosis. *Cureus*. 2025;17(1):e78319. <https://doi.org/10.7759/cureus.78319>.
33. **Allawzi A, Elajaili H, Redente EF, Nozik-Grayek E.** Oxidative Toxicology of Bleomycin: Role of the Extracellular Redox Environment. *Curr Opin Toxicol*. 2019;13:68-73. <https://doi.org/10.1016/j.cotox.2018.08.001>.